Annals of Hepatology 27 (2022) 100571

Contents lists available at ScienceDirect

Annals of Hepatology

journal homepage: www.elsevier.es/annalsofhepatology

Original article

Knockdown of long non-coding RNA LINC01006 represses the development of hepatocellular carcinoma by modulating the miR-194-5p/CADM1 axis

Zhaoxia Sun[a], Li Zhao[a], Shuang Wang[a], Honggang Wang[b,*]

[a] Department of Infectious Diseases, Weifang Yidu Central Hospital, No.4138, Linglongshan South Road, Qingzhou City, Weifang, Shandong 262500, China.
[b] Clinical Laboratory, Weifang People's Hospital, No.151, Guangwen Street, Kuiwen District, Weifang, Shandong 261041, China.

ARTICLE INFO

Article History:
Received 8 March 2021
Accepted 21 May 2021
Available online 27 October 2021

Keywords:
Hepatocellular carcinoma
LINC01006
miR-194-5p
CADM1

ABSTRACT

Introduction and objectives: Long non-coding RNAs (lncRNAs) have great potential as therapeutic targets in hepatocellular carcinoma (HCC). In this study, we aimed to uncover the function and molecular mechanism of long intergenic non-protein coding RNA 1006 (LINC01006) in HCC.
Materials and methods: Mice were injected with HCC cells in order to establish the HCC model. Quantitative reverse transcription polymerase chain reaction was used to determine the expression levels of LINC01006, cell adhesion molecule 1 (CADM1), and microRNA (miR)-194-5p in HCC tissues and cells. The cell proliferation, invasion, and migration abilities were assessed by 3-(4,5-dimethylthiazol-2-yl)-2,5-diphenyl-2H-tetrazolium bromide, transwell, and wound healing assays. The interrelation between LINC01006, miR-194-5p, and CADM1 was confirmed by a dual-luciferase reporter assay. Western blotting was employed to assess the relative protein expression level of CADM1.
Results: LINC01006 and CADM1 displayed upregulation, but miR-194-5p exhibited downregulation in HCC cells and tissues. Short hairpin (sh)-LINC01006 and miR-194-5p mimics repressed the proliferative, migratory, and invasive capacities of HCC cells, and injection of sh-LINC01006 restrained the growth of HCC tumours in mice. LINC01006 served as a competing endogenous RNA of miR-194-5p and was inversely correlated with miR-194-5p. CADM1 was targeted by miR-194-5p, inversely correlated with miR-194-5p, and positively associated with LINC01006. Furthermore, transfection of pcDNA-CADM1 or the miR-194-5p inhibitor reversed the suppressive effects of sh-LINC01006 on the proliferation, invasion, and migration abilities of HCC cells.
Conclusions: Downregulation of LINC01006 repressed the development of HCC by sponging miR-194-5p to modulate the expression of CADM1, implying its potential as a therapeutic target for HCC.

1. Introduction

Hepatocellular carcinoma (HCC), which is considered to be the third most fatal cancer worldwide, comprises 90% of all liver cancers [1]. As a rapidly growing and invasive tumour, HCC is chiefly induced by long-term liver injury caused by inherited metabolic disorders, viral hepatitis, excessive alcohol consumption, and toxin exposure [2]. The high probability of tumour metastasis and recurrence is the primary factor leading to the poor prognosis of patients with HCC [3]. There are many therapeutic modalities for HCC, including surgical options and ablative electrochemical therapies [4,5]. Currently, although HCC therapy has made great strides, the treatment effect on recurrent or metastatic HCC remains unsatisfactory, and the prevalence of HCC continues to rise [6–8]. Therefore, it is imperative to discover additional insights into the mechanism of HCC and exploit novel targets for HCC therapy.

Long non-coding RNAs (lncRNAs), which comprise over 200 nucleotides in length, are a subgroup of non-coding RNAs that exhibit limited or no protein-coding potential [9,10]. Several studies have confirmed the indispensable roles of lncRNAs in HCC [11–13]. A document from Zou et al. stated that silencing of lncRNA HLA complex group 18 suppresses the proliferation and migration of HCC cells while stimulating their apoptosis [11]. Another report from Wang et al. showed that knockdown of long intergenic non-protein coding RNA (LINC) 1134 inhibits the migration and invasion of HCC cells *in vitro* and restrains HCC liver metastasis *in vivo* [12]. A similar study by Wu et al. confirmed that lncRNA metallothionein 1J, pseudogene markedly impairs proliferation while also enhancing apoptosis in HCC cells [13].

* Corresponding author.
E-mail address: wanghonggang2130@163.com (H. Wang).

https://doi.org/10.1016/j.aohep.2021.100571

LINC01006, located on human chromosome 7q36.37, has been shown to be implicated in several cancers [14,15]. Downregulation of LINC01006 is closely associated with age, tumour size, tumour location, and venous invasion in gastric cancer [14]. Silencing of LINC01006 attenuates the proliferative, migratory, and invasive abilities of pancreatic cancer cells [15]. Nonetheless, there are few studies on the function and mechanism of LINC01006 in HCC.

MicroRNAs (miRNAs/miRs), which have a length of 19−24 nucleotides, are short single-stranded non-coding RNAs that can modulate gene expression at the post-transcriptional level [16]. In the past few years, increasing attention has been paid to miRNAs in the progression of HCC [17,18]. Wang et al. reported that upregulation of miR-302b represses the proliferation of HCC cells and the G1-S transition *in vitro* [17]. Li et al. indicated that inhibition of miR-221 restrains the proliferation, migration, and invasion of HCC cells [18]. LncRNAs can act as competing endogenous RNAs (ceRNAs) or sponges of miRNAs. Minichromosome maintenance complex component 3 associated protein antisense RNA 1 (MCM3AP-AS1) is known to contribute to the progression of HCC by targeting miR-194-5p [19]. X-inactive specific transcript (XIST) functions as a molecular sponge of miR-194-5p to accelerate HCC tumorigenesis [20]. In addition, miR-194-5p is reported to target numerous downstream genes that are involved in HCC progression, such as forkhead box A1 (FOXA1) [19], mitogen-activated protein kinase 1 (MAPK1) [20], and Wee1-like protein kinase [21]. More importantly, a recent study conducted by Niu et al. revealed that miR-194 interaction with cell adhesion molecule 1 (CADM1) affects the progression of HCC [22]. However, the interactions among LINC01006, miR-194-5p, and CADM1 in HCC have not yet been explored.

In the current study, we attempted to evaluate the expression and function of LINC01006 in HCC. Moreover, the molecular basis of LINC01006 in HCC progression was further investigated. We aimed to provide novel insights into the biological role of LINC01006 in HCC as well as a potential target for HCC treatment.

2. Materials and methods

2.1. HCC samples

From March 2018 to February 2019, paired HCC and adjacent normal tissues (n = 61) were acquired from patients who underwent hepatectomy. None of the HCC patients received any chemotherapy or embolotherapy before surgery. The tissue samples were affirmed by two histopathologists. The present study was approved by the ethics committee of Weifang Yidu Central Hospital on the basis of the Declaration of Helsinki. Each participant enrolled in this research provided written informed consent before the surgical operation.

2.2. Cell culture

The human immortalised liver cell line (MIHA) and human HCC cell lines (Huh7, SNU-398, Hep3B, and Sk-Hep1) were purchased from the American Type Culture Collection (Manassas, VA, USA). The cells were cultured in Dulbecco's Modified Eagle's Medium (DMEM; Gibco, Grand Island, NY, USA) supplemented with 10% foetal bovine serum (FBS; Gibco) and antibiotics (100 U/mL penicillin and 100 μg/mL streptomycin) at 37 °C with 5% CO_2.

2.3. Quantitative real-time polymerase chain reaction (qRT-PCR)

Trizol reagent (Sangon Biotech, Shanghai, China) was used for RNA isolation. Total RNA was reverse transcribed into complementary DNA using an M-MLV Reverse Transcriptase kit (Sangon Biotech). The qRT-PCR assay was implemented using SYBR® Premix Ex Taq™ II (Takara, Dalian, China). The PCR 额ing conditions were as follows: 94 °C for 5 min, followed by 40 cycles of 94 °C for 30 s, 60 °C for 20 s, and 72 °C for 5 min. All primers were purchased from Invitrogen (Carlsbad, CA, USA), and the primer sequences are shown in Table 1. The relative expression levels of LINC01006, miR-194-5p, and CADM1 were calculated using the $2^{-\Delta\Delta ct}$ method. Glyceraldehyde 3-phosphate dehydrogenase was used as an internal reference.

2.4. Cell transfection

Short hairpin RNAs (shRNAs) against LINC01006 (sh-LINC01006-1 and sh-LINC01006-2), shRNA negative control (sh-NC), miR-NC, miR-194-5p mimics, miR-194-5p inhibitor, pcDNA-NC, and pcDNA-CADM1 were purchased from RiboBio Company (Beijing, China). Next, the above factors were transfected into Hep3B and Sk-Hep1 cells using Lipofectamine 3000 (Invitrogen) for 48 h according to the provided protocol.

2.5. Dual-luciferase reporter (DLR) assay

The 3′-untranslated region (UTR) of LINC01006 or CADM1 harbouring the binding sequence of miR-194-5p was introduced into the pGL3 luciferase reporter vector (Promega, Madison, WI, USA), forming the LINC01006 wild type (WT) or CADM1 WT. Analogously, the 3′-UTR segment of LINC01006 or CADM1, including the mutated binding sequence of miR-194-5p, was introduced into the pGL3 luciferase reporter vector (Promega), generating the LINC01006 mutant (MUT) or CADM1 MUT. The above reporters, along with miR-194-5p mimics or miR-NC, were transfected into cells using Lipofectamine 3000 (Invitrogen). After transfection for 48 h, relative luciferase activity was measured with a DLR assay system (Promega).

2.6. 3-(4,5-dimethylthiazol-2-yl)-2,5-diphenyl-2H-tetrazolium bromide (MTT) assay

Cells were seeded into 96-well plates at a density of 6,000 cells/well. At 0, 24, 48, 72, and 96 h after incubation, MTT (10 μL; Sigma-Aldrich, St. Louis, MO, USA) was added, and the cells were incubated at 37 °C for another 4 h. At the end of the culture, 150 μL dimethyl sulfoxide was added. The optical density at 490 nm was measured with an FL600 fluorescence plate reader (Bio-Rad, Hercules, CA, USA).

2.7. Wound healing assay

Cells were seeded into 6-well plates at a density of 6×10^4 cells/well and cultured with DMEM containing 10% FBS until the cell monolayer was generated. Unilaminar cells were scratched with a 10 μL sterile pipette tip. Then, PBS was added to remove the scratched cells. The cells were then cultured in serum-free medium at 37°C. After culturing for 24 h, the migration distance of the cell scratch region was examined under an inverted microscope (TE2000; Nikon,

Table 1
Primers for qRT-PCR in this study.

Gene	Forward	Reverse
LINC01006	5'-TTTGTGGTGGTGAAGACGTG-3'	5'-TCCTCAAGAATAAGGAACATAGGC-3'
MiR-194-5p	5'-GCCGCTGTAACAGCAACTCCAT-3'	5'-GTGCAGGGTCCGAGGT-3'
CADM1	5'-TGCTGTGCTTGCTCATCATTCT-3'	5'- TCTGCGTCTGCTGCGTCAT-3'
GAPDH	5'-CAGGAGGCATTGCTGATGAT -3'	5'-GAAGGCTGGGGCTCATTT-3'

Tokyo, Japan). The formula for calculating the wound healing rate was as follows: (1−24 h scratch width/0 h scratch width) × 100.

2.8. Transwell assay

The cell invasion capacity was determined using a transwell chamber coated with Matrigel (BD Biosciences, Sparks, MD, USA). First, cells in serum-free medium were shifted to the upper chamber (BD Biosciences). The lower chamber was loaded with 600 μL DMEM containing 10% FBS. After incubation for 24 h, the transwell chamber was removed. Cells in the upper compartment were sponged with cotton swabs, and cells in the lower compartment were stained with 0.1% crystal violet for 5 min. After washing with PBS, the invasive ability of the cells was evaluated by counting the number of invading cells under a fluorescence microscope (TE2000; Nikon).

2.9. Western blot

Total cells were lysed using radioimmunoprecipitation assay buffer (Thermo Fisher Scientific, Waltham, MA, USA). Protein samples were isolated by 10% sodium dodecyl sulphate-polyacrylamide gel electrophoresis, transferred to polyvinylidene difluoride membranes, and blocked with 5% non-fat milk. The membranes were then incubated with the anti-CADM1 (1:1000, ab216585; Abcam, Cambridge, MA, USA) and anti-β-tubulin (1:500, ab6046; Abcam) primary antibodies overnight at 4°C. After washing with tris-buffered saline-Tween 20, the secondary antibody (1:2000, ab6747; Abcam) was supplemented and cultured with the protein samples at 37 °C for 1 h. The blot signals were visualised using electrochemiluminescence reagents (Millipore, Plano, TX, USA). The relative expression of CADM1 over the β-tubulin band was quantified using a Gel-Pro Analyser (Media Cybernetics, Rockville, MD, USA).

2.10. Nude mouse tumorigenesis assay

All animal experiments were approved by the animal ethics committee of our hospital and abided by the National Institutes of Health Guide for the Care and Use of Laboratory Animals. Four-week-old male BALB/C nude mice were purchased from the National Laboratory Animal Center (Beijing, China) and divided into two groups (n = 5 per group). Hep3B cells (5×10^6) transfected with the lentivirus vector of sh-LINC01006-1 (Lv-sh-LINC01006-1) or the lentivirus vector of sh-NC (Lv-sh-NC) were subcutaneously implanted into the right flank of the nude mice at 100 μL cell suspension per injection as previously described [23]. Tumour volumes were gauged once every 5 days and calculated using the following formula: $(A \times B^2) / 2$ (A, the longest diameter; B, the shortest diameter). On the 30th day after injection, the mice were anaesthetized with pentobarbital sodium (50 mg/kg) and sacrificed. The tumours were then dissected and weighed.

2.11. Statistical analysis

In vitro experiments were repeated three times. Additionally, the MTT assay, DLR assay, and qRT-PCR were performed in triplicate (3 × 3). In vivo experiments were performed using five mice in each group. Data were analysed using SPSS Statistics 22.0 software (IBM SPSS, Armonk, NY, USA) and are presented as means ± standard deviations. The Student's t-test was used to compare differences between two groups. A one-way analysis of variance was used to analyse differences among multiple groups, and Tukey's multiple comparisons test was used for pairwise comparisons. The correlations between two genes were analysed using the Pearson correlation test. Differences were considered statistically significant at $P < 0.05$.

3. Results

3.1. LINC01006 is highly expressed in HCC tissues and cells

To determine the role of LINC01006 in HCC, we determined the expression of LINC01006 in tumour tissues from HCC patients and in HCC cell lines. The qRT-PCR results showed that the relative expression level of LINC01006 in tumour tissues was distinctly elevated compared to that in adjacent normal tissues ($P < 0.001$; Fig. 1A). Next, to determine the clinical significance of LINC01006 in HCC, we analysed the

Table 2
Clinical parameters of the patients with HCC who were included in this study.

Variable	Total	LINC01006 expression		P-value
		Low(30)	High(31)	
Gender				0.662
Male	39	20	19	
Female	22	10	12	
Age				0.684
< 60years	35	18	17	
≥ 60 years	26	12	14	
Diameter				0.332
< 6 cm	39	21	18	
≥ 6 cm	22	9	13	
Metastasis				0.015*
NO	31	20	11	
YES	30	10	20	
TNM stage				0.028*
I/II	24	16	8	
III/IV	37	14	23	

Note: *$P < 0.05$, WHO: world health organization, TNM : tumour node metastasis.

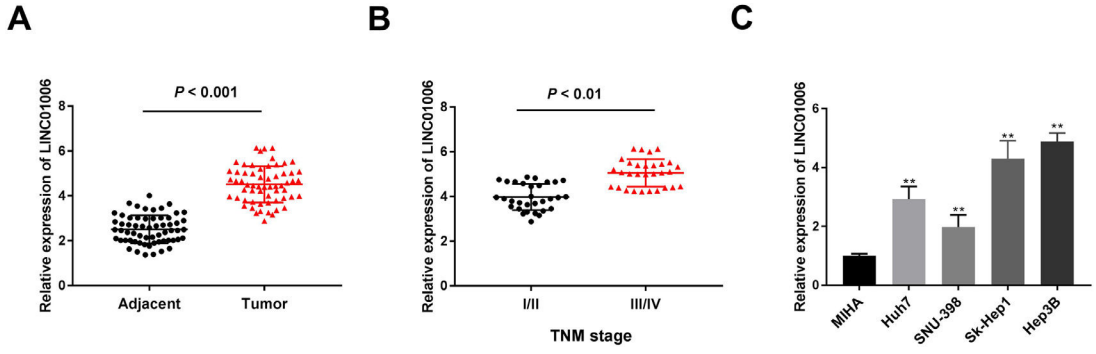

Fig. 1. LINC01006 was highly expressed in hepatocellular carcinoma (HCC) tissues and HCC cells. (A) Relative expression of LINC01006 in tumour tissues and adjacent normal tissues was determined by quantitative real-time polymerase chain reaction (qRT-PCR). $P < 0.001$, vs. Adjacent normal tissues. (B) Relative expression of LINC01006 at tumour node metastasis (TNM) stage I/II and TNM stage III/IV was determined by qRT-PCR in tumour. $P < 0.01$, vs. I/II. (C) Relative expression of LINC01006 in HepG2, SMMC-7721, Hep3B, Sk-Hep1 and LO2 cells was determined by qRT-PCR. $^{**}P < 0.01$, vs. LO2.

relationships between clinicopathological features and the expression of LINC01006 in HCC cases. We discovered that LINC01006 was closely associated with metastasis and tumour node metastasis (TNM) stage (Table 2). The relative expression of LINC01006 in HCC patients at TNM stage III-IV was boosted compared to that in patients at TNM stage I-II ($P < 0.01$; Fig. 1B). We also observed that LINC01006 was upregulated in HCC cell lines (Huh7, SNU-398, Hep3B, and Sk-Hep1) compared to MIHA cells (all $P < 0.01$; Fig. 1C). Among them, Hep3B and Sk-Hep1 were selected for the subsequent trials because of the relatively high expression levels of LINC01006.

3.2. Downregulation of LINC01006 suppresses the proliferation, migration, and invasion of HCC cells and represses HCC tumour growth in mice

Next, we probed the potential role of LINC01006 in HCC cells. First, we silenced LINC01006 using sh-LINC01006-1 or sh-LINC01006-2 in Hep3B and Sk-Hep1 cells. As shown in Fig. 2A, the expression of LINC01006 was markedly reduced by sh-LINC01006-1 or sh-LINC01006-2 in Hep3B and Sk-Hep1 cells ($P < 0.01$), and sh-LINC01006-1 was selected for subsequent experiments on account of its relatively high knockdown efficiency. The results of the MTT assay indicated that the viability of Hep3B and Sk-Hep1 cells in the sh-LINC01006-1 group was lower than that in the sh-NC group (all $P < 0.01$; Fig. 2B). The wound healing assay showed that the wound healing rate of Hep3B and Sk-Hep1 cells was decreased by the knockdown of LINC01006 (all $P < 0.01$; Fig. 2C). The transwell assay demonstrated that the number of invading cells was diminished by the knockdown of LINC01006 in Hep3B and Sk-Hep1 cells (all $P < 0.01$; Fig. 2D). To elucidate the biological role of LINC01006 in HCC *in vivo*, we performed a mouse tumorigenesis assay. As shown in Fig. 2E, the tumour volume in the Lv-sh-LINC01006-1 group was dramatically reduced on the 20th, 25th, and 30th days after injection relative to the Lv-sh-NC group ($P < 0.01$; Fig. 2E). Moreover, the tumour weight

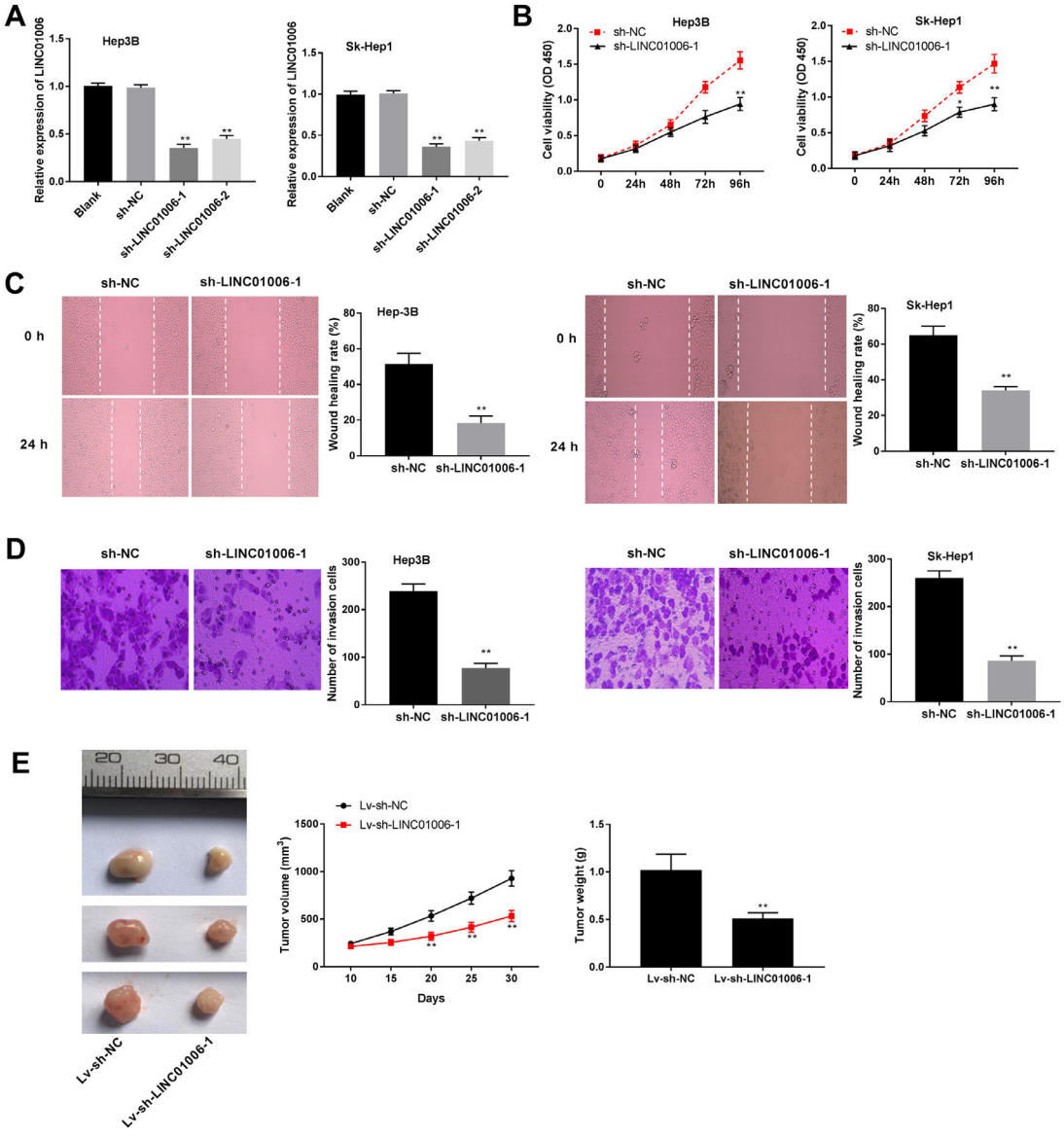

Fig. 2. Knockdown of LINC01006 suppressed cell viability, migration and invasion in hepatocellular carcinoma (HCC) cells, and repressed tumour growth in mice. (A) Relative expression of LINC01006 in Hep3B and Sk-Hep1 cells after transfection with shRNA-LINC01006-1 (sh-LINC01006-1), sh-LINC01006-2 and shRNA negative control (sh-NC) was detected by quantitative real-time polymerase chain reaction (qRT-PCR). $^{**}P < 0.01$, vs. sh-NC. (B) Cell viability in Hep3B and Sk-Hep1 cells was detected by 3-(4, 5-Dimethyl-2-Thiazolyl)-2, 5-Diphenyl-2-H-Tetrazolium Bromide (MTT) assay. $^{*}P < 0.05$, $^{**}P < 0.01$, vs. sh-NC. (C) Wound healing rate of Hep3B and Sk-Hep1 cells was detected by wound healing assay. $^{**}P < 0.01$, vs. sh-NC. (D) Number of invasion cells in Hep3B and Sk-Hep1 cells was detected by transwell assay. $^{**}P < 0.01$, vs. sh-NC. (E) Three representative images of solid tumours, and the growth of tumours in mice injected with Hep3B cells transfected with Lentivirus vector carrying sh-LINC01006-1 (Lv-sh-LINC01006-1) or Lv-sh-NC. $^{**}P < 0.01$, vs. Lv-sh-NC.

in the Lv-sh-LINC01006-1 group was also evidently reduced compared to the Lv-sh-NC group on the 30th day after injection ($P < 0.01$; Fig. 2E).

3.3. LINC01006 acts as a sponge of miR-194-5p

To gain mechanistic insight into LINC01006, we predicted its target using the LncBase Predicted v2 database. The results illustrated that miR-194-5p shared complementary binding to LINC01006 (Fig. 3A). Meanwhile, miR-194-5p was upregulated by the transfection of sh-LINC01006-1 into Hep3B and Sk-Hep1 cells (all $P < 0.01$; Fig. 3B), suggesting a negative modulation loop between miR-194-5p and LINC01006 in human HCC cells. To test the association between miR-194-5p and LINC01006, a DLR assay was conducted, which showed that upregulation of miR-194-5p reduced the relative luciferase activity of Hep3B and Sk-Hep1 cells transfected with the LINC01006 WT reporter but had no significant impact on the relative luciferase activity of Hep3B and Sk-Hep1 cells transfected with LINC01006 MUT ($P < 0.01$; Fig. 3C). In addition, miR-194-5p was notably diminished in tumour tissues compared to adjacent normal tissues ($P < 0.001$; Fig. 3D). The outcome of Pearson correlation analysis indicated that there was an inverse correlation between miR-194-5p and LINC01006 in human HCC tissues ($P = 0.0009$, $r = -0.4155$; Fig. 3E). In addition, the expression of miR-194-5p was determined in HCC cell lines. As illustrated in Fig. 3F, we observed decreased expression of miR-194-5p in HCC cell lines compared to MIHA cells ($P < 0.01$).

3.4. Overexpression of miR-194-5p represses cell viability, migration, and invasion in HCC cells

Subsequently, we examined the function of miR-194-5p in HCC cells. As illustrated in Fig. 4A, we observed that the expression of miR-194-5p in Hep3B and Sk-Hep1 cells was increased by transfection with miR-194a-5p mimics and decreased by the miR-194a-5p inhibitor ($P < 0.01$). The cell viability of Hep3B and Sk-Hep1 cells was decreased by miR-194-5p overexpression (all $P < 0.01$; Fig. 4B). In addition, the migratory and invasive abilities of Hep3B and Sk-Hep1 cells were repressed by overexpression of miR-194-5p (all $P < 0.01$; Fig. 4C and D).

3.5. CADM1 is the target of miR-194-5p

In order to identify the downstream target of miR-194-5p, we performed a prediction using StarBase. The results showed that there were binding sites between CADM1 and miR-194-5p (Fig. 5A). To confirm this prediction, a DLR assay was performed. The results revealed that the relative luciferase activity of Hep3B and Sk-Hep1 cells was visibly decreased by co-transfection with the CADM1 WT reporter and miR-194-5p mimics, whereas the relative luciferase activity of Hep3B and Sk-Hep1 cells was not significantly different after co-transfection with miR-194-5p mimics and the CADM1 MUT reporter ($P < 0.01$; Fig. 5B). Western blot analysis showed that CADM1 expression was distinctly reduced by miR-194-5p overexpression in Hep3B and Sk-Hep1 cells ($P < 0.01$; Fig. 5C). Data from The Cancer Genome Atlas database indicated that expression of CADM1 was augmented in HCC tissues compared to adjacent normal

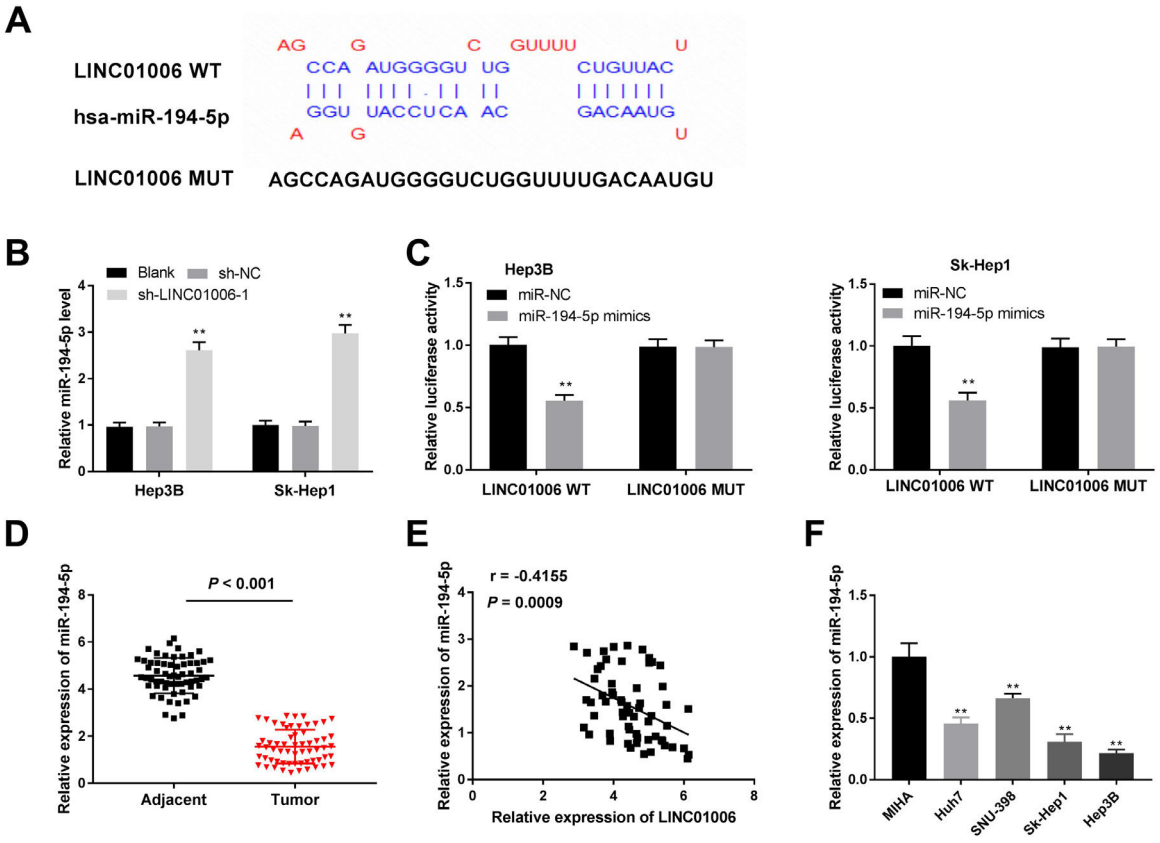

Fig. 3. LINC01006 acted as a sponge of miR-194-5p. (A) The binding sequence between LINC01006 and miR-194-5p was predicted by LncBase Predicted v.2. (B) Relative expression of miR-194-5p in Hep3B and Sk-Hep1 cells was detected by quantitative real-time polymerase chain reaction (qRT-PCR). $^{**}P < 0.01$, vs. sh-NC. (C) The interaction between LINC01006 and miR-194-5p in Hep3B and Sk-Hep1 cells was confirmed by dual-luciferase reporter (DLR) assay. $^{**}P < 0.01$, vs. miR-negative control (NC). (D) Relative expression of miR-194-5p was detected by qRT-PCR in tumour tissues and adjacent normal tissues. $P < 0.001$, vs. Adjacent normal tissues. (E) Correlation analysis of LINC01006 and miR-194-5p in hepatocellular carcinoma (HCC) tissues. $P = 0.0009$. (F) Relative expression of miR-194-5p in HepG2, Hep3B, SMMC-7721, Sk-Hep1 and LO2 cells was determined by qRT-PCR. $^{**}P < 0.01$, vs. LO2.

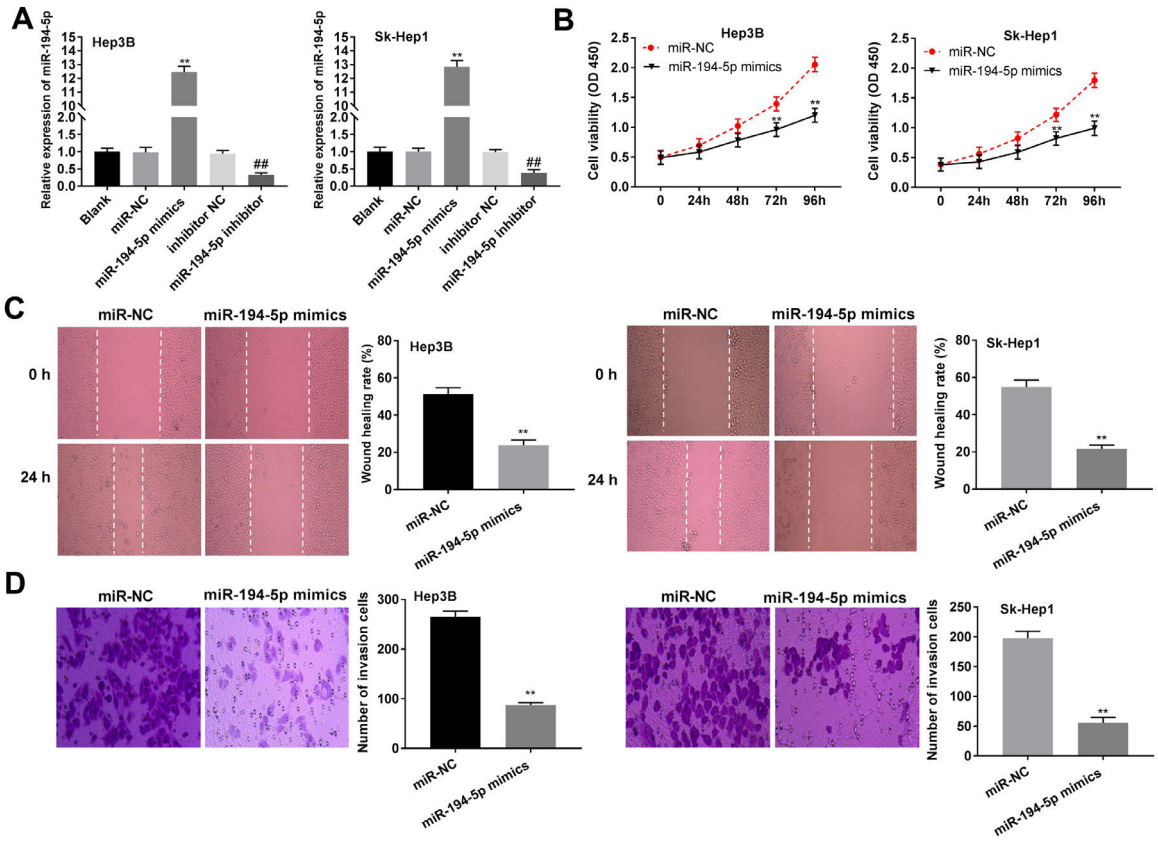

Fig. 4. Overexpression of miR-194-5p repressed cell viability, migration and invasion in hepatocellular carcinoma (HCC) cells. (A) Relative expression of miR-194-5p in Hep3B and Sk-Hep1 cells was detected by quantitative real-time polymerase chain reaction (qRT-PCR). $^{**}P < 0.01$, vs. miR-NC. $^{\#\#}P < 0.01$, vs. inhibitor NC. (B) Cell viability in Hep3B and Sk-Hep1 cells was determined by 3-(4, 5-Dimethyl-2-Thiazolyl)-2, 5-Diphenyl-2-H-Tetrazolium Bromide (MTT) assay. $^{**}P < 0.01$, vs. miR-negative control (NC). (C) Wound healing rate of Hep3B and Sk-Hep1 cells was determined by wound healing assay. $^{**}P < 0.01$, vs. miR-NC. (D) Number of invasion cells in Hep3B and Sk-Hep1 cells was detected by transwell assay. $^{**}P < 0.01$, vs. miR-NC.

tissues ($P < 0.05$; Fig. 5D). The results from qRT-PCR showed that CADM1 was also elevated in tumour tissues relative to that in adjacent normal tissues ($P < 0.001$; Fig. 5E). Pearson correlation analysis demonstrated that LINC01006 was positively correlated with CADM1 in human HCC tissues ($P = 0.0008$, $r = 0.4190$; Fig. 5F), and miR-194-5p was inversely correlated with CADM1 in human HCC tissues ($P = 0.0004$, $r = -0.4389$; Fig. 5G). Moreover, the results of the western blot assay demonstrated that the protein level of CADM1 was significantly elevated in HCC cell lines compared to that in MIHA cells ($P < 0.01$; Fig. 5H).

3.6. Downregulation of LINC01006 represses cell invasion, migration, and proliferation by sponging miR-194-5p to modulate the expression of CADM1

To further validate the relationships among LINC01006, miR-194-5p, and CADM1, sh-LINC01006-1 or sh-LINC01006-1 + miR-194a-5p inhibitor was transfected into Hep3B cells to determine the protein level of CADM1. As presented in Fig. 6A, the CADM1 protein level was downregulated by sh-LINC01006-1 ($P < 0.01$), whereas transfection with miR-194a-5p reversed the inhibitory effect of sh-LINC01006-1 on the CADM1 protein level ($P < 0.05$). Next, the transfection efficiency of pcDNA-CADM1 was determined. We found that CADM1 expression was significantly elevated in Hep3B cells transfected with pcDNA-CADM1 ($P < 0.01$, Fig. 6B), which suggested that pcDNA-CADM1 was transfected successfully. Next, we carried out rescue experiments. We discovered that the addition of sh-LINC01006-1 significantly decreased cell viability in Hep3B cells ($P < 0.01$), and the inhibitory effect of sh-LINC01006-1 on cell viability was reversed by the addition of pcDNA-CADM1 or miR-194-5p inhibitor in Hep3B cells (all $P < 0.01$; Fig. 6C). Furthermore, the cell migration and invasion abilities were restrained by sh-LINC01006-1 in Hep3B cells (all $P < 0.01$), and the suppressive effects of sh-LINC01006-1 on the migratory and invasive abilities of Hep3B cells were reversed by pcDNA-CADM1 or the miR-194-5p inhibitor (all $P < 0.01$; Fig. 6D and E).

4. Discussion

HCC is regarded as a common hepatic malignancy worldwide that continues to increase in prevalence [24, 25]. Previous studies have revealed upregulation of several lncRNAs in HCC, including myocardial infarction-associated transcript [26], lncRNA activated by transforming growth factor-β [27] and HOX antisense intergenic RNA [28]. Consistent with the above studies, we observed that LINC01006 was augmented in HCC tissues and cells compared to their controls, implying that LINC01006 is involved in HCC. Moreover, a prior study stated that LINC01006 is relevant to tumour location, tumour size, venous invasion, and age in gastric cancer [14]. Similarly, we found that LINC01006 was associated with metastasis and TNM stage. Its association with metastasis also indicates that LINC01006 may be applied as a tool for predicting prognosis, given that metastasis is relevant to the poor prognosis of patients with HCC [3].

Recent studies have shown that LINC01006 plays a critical role in pancreatic cancer [15, 29]. Ma et al. revealed that overexpression of LINC01006 significantly contributes to enhancing the proliferation, migration, and invasion of prostate cancer cells [29]. Zhang et al. stated that LINC01006 knockdown represses the cell invasion, migration, and proliferation abilities in pancreatic cancer [15]. Similarly, we discovered that the knockdown of LINC01006 also represses cell

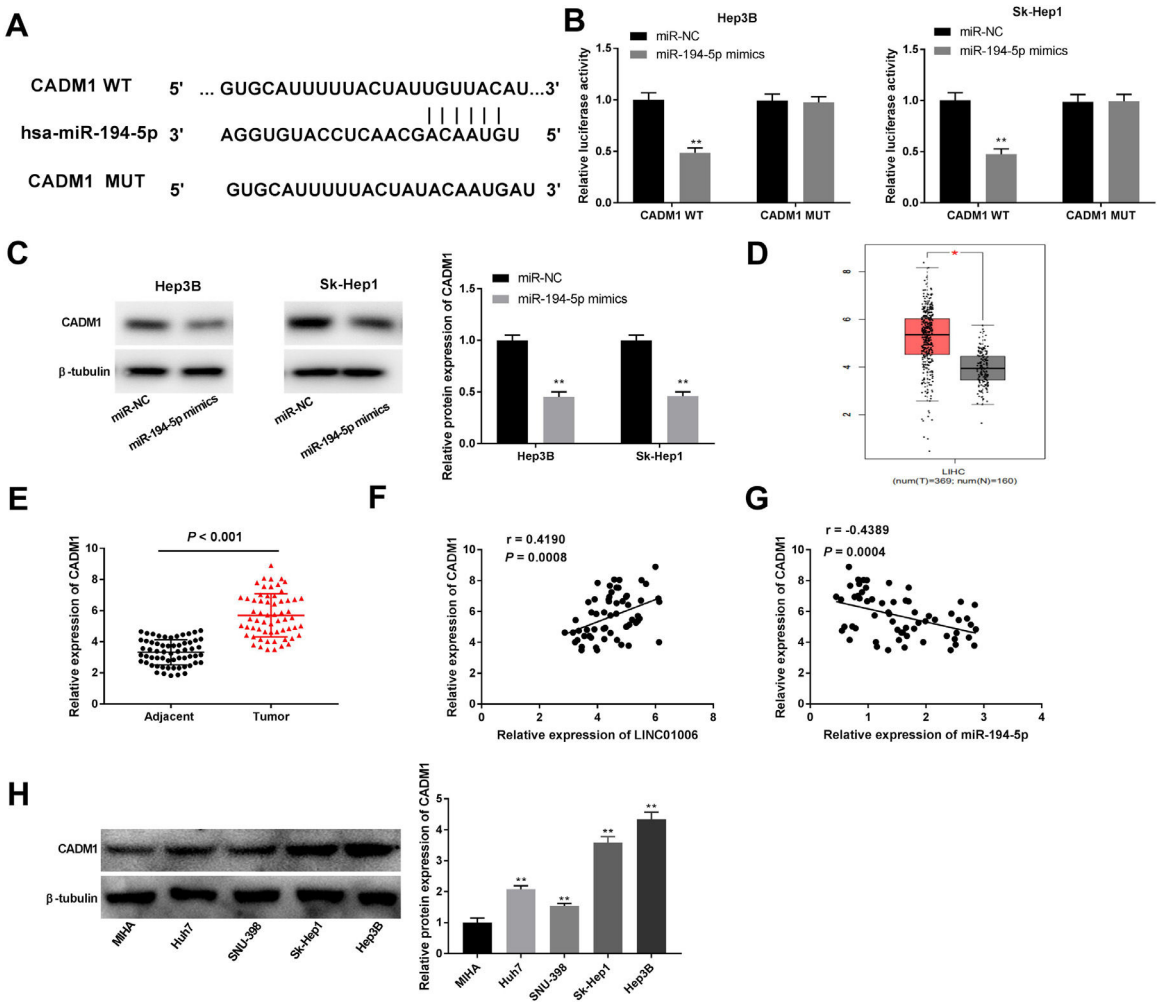

Fig. 5. CADM1 was target gene of miR-194-5p. (A) The binding sites between CADM1 and miR-194-5p were predicted by LncBase Predicted v.2. (B) Dual-luciferase reporter (DLR) assay was used for confirming the relationship between miR-194-5p and CADM1 in Hep3B and Sk-Hep1 cells. $^{**}P < 0.01$, vs. miR-negative control (NC). (C) Relative protein expression of CADM1 in Hep3B and Sk-Hep1 cells was detected by western blot. $^{**}P < 0.01$, vs. miR-NC. (D) Relative expression of CADM1 in hepatocellular carcinoma (HCC) tissues and non-cancerous tissues from the cancer genome atlas (TCGA) database. $^{*}P < 0.05$, vs. Non-cancerous tissues. LIHC: liver hepatocellular carcinoma. (E) Quantitative real-time polymerase chain reaction (qRT-PCR) was used to detect relative expression of CADM1 in tumour tissues and adjacent normal tissues. $P < 0.001$, vs. Adjacent normal tissues. (F) The relationship between LINC01006 and CADM1 in HCC tissues was analyzed by Pearson's correlation analysis. (G) The relationship between CADM1 and miR-194-5p in HCC tissues was analyzed by Pearson's correlation analysis. (H) Relative expression of CADM1 in HepG2, Hep3B, SMMC-7721, Sk-Hep1 and LO2 cells was determined by western blot. $^{**}P < 0.01$, vs. LO2.

proliferation, invasion, and migration in HCC. Additionally, in nude mouse xenograft models, downregulation of LINC01006 remarkably repressed HCC tumour growth. These findings indicate that LINC01006 may act as a novel target for HCC therapy.

Previous studies have shown that lncRNAs can serve as ceRNAs to sponge miRNAs in diverse cancers, including HCC [30]. EPB41L4A-AS2-miR-301a-5p [31], PCAT-1-miR-215 [32] and MALAT1-miR-200a [33] have been verified in HCC. Here, we validated that lncRNA LINC01006 functions as a ceRNA to sponge miR-194-5p and that it is inversely correlated with miR-194-5p. In addition, downregulation of miR-194-5p has previously been demonstrated to participate in the progression of HCC cells [19,20]. Downregulation of miR-194-5p was affirmed in HCC tissues compared to paracancerous tissues, and MCM3AP-AS1 was revealed to exert an oncogenic role by targeting miR-194-5p in HCC [19]. MiR-194-5p was shown to be diminished in HCC tissues compared to non-tumour tissues, and overexpression of miR-194-5p appeared to suppress the proliferation and invasion of HCC cells [20]. Similarly, we discovered that upregulation of miR-194-5p attenuates the cell proliferation, invasion, and migration abilities in HCC cells. We also found that the miR-194-5p inhibitor reversed the suppressive effects of sh-LINC01006 on the viability, invasion, and migration of HCC cells. Taken together, we inferred that sh-LINC01006 fulfils a tumour suppressor role by targeting miR-194-5p in HCC.

CADM1, also known as tumour suppressor in lung cancer 1, encodes a 442 amino acid protein that contains a cytoplasmic domain, an extracellular domain, and a transmembrane domain [34,35]. Aberrant expression of CADM1 has been demonstrated to play a notable role in the progression of HCC [36,37]. Sun et al. affirmed that suppression of CADM1 can stimulate the migration and invasion of HCC cells [38]. Zhang et al. declared that upregulation of CADM1 represses the tumorigenicity of HCC both *in vitro* and *in vivo* [37]. In the current study, CADM1 was found to have increased expression in HCC cells and tissues compared to their controls, suggesting that CADM1 may be implicated in the development of HCC. Moreover, CADM1 has also been reported to act as the downstream target of other miRNAs in HCC, such as miR-1246 [38] and miR-10b [39]. Here, CADM1 was the target of miR-194-5p, and Pearson correlation analysis revealed that there was an inverse association between CADM1 and miR-194-5p in HCC tissues. In view of the above findings, we speculated that miR-194-5p acted as a tumour suppressor by targeting CADM1 in HCC. We also found that CADM1 was inversely correlated with LINC01006,

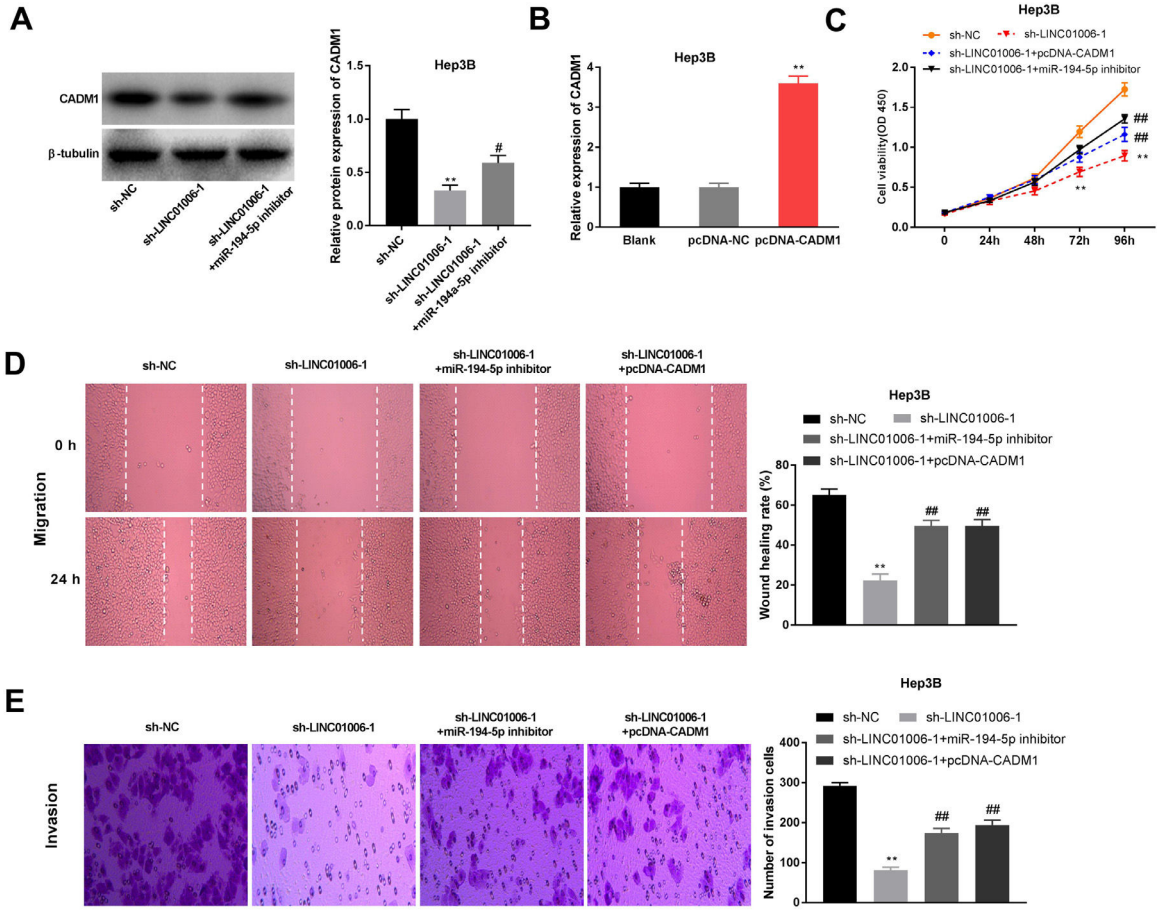

Fig. 6. Knockdown of LINC01006 inhibited cell invasion, migration and proliferation by sponging miR-194-5p to modulate the expression of CADM1. (A) Relative expression of CADM1 in Hep3B cells was detected by quantitative real-time polymerase chain reaction (qRT-PCR). $^{**}P < 0.01$, vs. pcDNA-NC. (B) Cell viability in Hep3B cells was determined by 3-(4, 5-Dimethyl-2-Thiazolyl)-2, 5-Diphenyl-2-H-Tetrazolium Bromide (MTT) assay. $^{**}P < 0.01$, vs. sh-negative control (NC). $^{\#\#}P < 0.01$, vs. sh-LINC01006-1. (C) Wound healing rate of Hep3B cells was determined by wound healing assay. $^{**}P < 0.01$, vs. sh-NC. $^{\#\#}P < 0.01$, vs. sh-LINC01006-1. (D) Number of invasion cells in Hep3B cells was detected by transwell assay. $^{**}P < 0.01$, vs. sh-NC. $^{\#\#}P < 0.01$, vs. sh-LINC01006-1.

and the suppressive effects of sh-LINC01006 on the viability, migration, and invasion of HCC cells were reversed by pcDNA-CADM1. We found that sh-LINC01006 may repress the development of HCC by modulating the miR-194-5p/CADM1 axis. In addition, LINC01006 interaction with other regulatory axes in pancreatic cancer and prostate cancer has previously been reported [15,29]. Zhang et al. demonstrated that the LINC01006/miR-2682-5p/HOXB8 axis accelerates the tumorigenesis of pancreatic cancer and thus may be a treatment target [15]. Ma et al. showed that LINC01006 is involved in the enhancement of cell proliferation, migration, and invasion in prostate cancer via interaction with the miR-34a-5p/DAAM1 axis [29]. Meanwhile, the functions of the miR-194-5p/FOXA1 [19] and miR-194-5p/MAPK1 axes [20] as well as the CADM1-Rb-E2F [37] and CADM1-STAT3 pathways [40] have been confirmed in HCC. We speculated that these downstream targets and pathways may also be involved in the regulatory mechanism of LINC01006 in HCC.

To conclude, our results uncovered that LINC01006 is upregulated in HCC tissues and cells. LINC01006 directly interacts with miR-194-5p, and CADM1 is targeted by miR-194-5p. Mechanistically, sh-LINC01006 serves as a tumour suppressor lncRNA by sponging miR-194-5p and subsequently modulating the expression of CADM1. Thus, our results illustrate that LINC01006 may be a promising target for HCC therapy.

Availability of data and materials

The datasets used and/or analyzed during the current study are available from the corresponding author on reasonable request

Ethics approval and consent to participate

The present study was authorized by the ethics committee of Weifang Yidu Central Hospital on the basis of the Declaration of Helsinki. Each participant enrolled in this research had written informed consent before surgical operation.

Consent for publication

Not applicable

Funding

Funding information is not applicable.

Conflicts of interest

The authors have no conflicts of interest to declare

Long non-coding RNAs (lncRNAs), hepatocellular carcinoma (HCC),long intergenic non-protein coding RNA 1006 (LINC01006), cell adhesion molecule 1 (CADM1), microRNA (miR), long intergenic non-protein coding RNA (LINC),MicroRNAs (miRNAs/miRs), competing endogenous RNAs (ceRNAs), X-inactive specific transcript (XIST), forkhead box A1 (FOXA1), mitogen-activated protein kinase 1 (MAPK1), Quantitative real-time polymerase chain reaction (qRT-PCR),Short hairpin RNAs (shRNAs), shRNA negative control (sh-NC), Dual-luciferase reporter (DLR).

CRediT authorship contribution statement

Zhaoxia Sun: Visualization, Data curation, Formal analysis. **Li Zhao:** Investigation, Writing – original draft, Writing – review & editing. **Shuang Wang:** Visualization, Data curation, Formal analysis, Writing – review & editing. **Honggang Wang:** Investigation, Writing – original draft, Writing – review & editing.

Acknowledgments

Not applicable.

References

[1] Bosch FX, Ribes J, Cleries R, Diaz M. Epidemiology of hepatocellular carcinoma. Clin Liver Dis 2005;9:191–211 v. doi: S1089-3261(04)00130-8 [pii]. https://doi.org/10.1016/j.cld.2004.12.009.
[2] Farazi PA, DePinho RA. Hepatocellular carcinoma pathogenesis: from genes to environment. Nat Rev Cancer 2006;6:674–87 doi: nrc1934 [pii]. https://doi.org/10.1038/nrc1934.
[3] Dika IE, Abou-Alfa GK. Treatment options after sorafenib failure in patients with hepatocellular carcinoma. Clin Mol Hepatol 2017;23:273–9 cmh.2017.0108 [pii]. https://doi.org/10.3350/cmh.2017.0108.
[4] Hartke J, Johnson M, Ghabril M. The diagnosis and treatment of hepatocellular carcinoma. Semin Diagn Pathol 2017;34:153–9 S0740-2570(16)30117-4 [pii]. https://doi.org/10.1053/j.semdp.2016.12.011.
[5] Innes H, Barclay ST, Hayes PC, Fraser A, Dillon JF, Stanley A, et al. The risk of hepatocellular carcinoma in cirrhotic patients with hepatitis C and sustained viral response: Role of the treatment regimen. J Hepatol 2018;68:646–54 doi: S0168-8278(17)32429-7 [pii]. https://doi.org/10.1016/j.jhep.2017.10.033.
[6] Tejeda-Maldonado J, Garcia-Juarez I, Aguirre-Valadez J, Gonzalez-Aguirre A, Vilatoba-Chapa M, Armengol-Alonso A, et al. Diagnosis and treatment of hepatocellular carcinoma: an update. World J Hepatol 2015;7:362–76. https://doi.org/10.4254/wjh.v7.i3.362.
[7] Llovet JM, Bustamante J, Castells A, Vilana R, Ayuso Mdel C, Sala M, et al. Natural history of untreated nonsurgical hepatocellular carcinoma: rationale for the design and evaluation of therapeutic trials. Hepatology 1999;29:62–7 doi: S0270913999000105 [pii]. https://doi.org/10.1002/hep.510290145.
[8] Bruix J, Boix L, Sala M, Llovet JM. Focus on hepatocellular carcinoma. Cancer Cell 2004;5:215–9 doi: S1535610804000583 [pii]. https://doi.org/10.1016/s1535-6108(04)00058-3.
[9] Mercer TR, Dinger ME, Mattick JS. Long non-coding RNAs: insights into functions. Nat Rev Genet 2009;10:155–9 nrg2521 [pii]. https://doi.org/10.1038/nrg2521.
[10] Ponting CP, Oliver PL, Reik W. Evolution and functions of long noncoding RNAs. Cell 2009;136:629–41 S0092-8674(09)00142-1 [pii]. https://doi.org/10.1016/j.cell.2009.02.006.
[11] Zou Y, Sun Z, Sun S. LncRNA HCG18 contributes to the progression of hepatocellular carcinoma via miR-214-3p/CENPM axis. J Biochem 2020 doi: mvaa073 [pii] [pii]. https://doi.org/10.1093/jb/mvaa0735871354.
[12] Wang C, Chen Y, Chen K, Zhang L. Long noncoding RNA LINC01134 promotes hepatocellular carcinoma metastasis via activating AKT1S1 and NF-kappaB signaling. Front Cell Dev Biol 2020;8:429. https://doi.org/10.3389/fcell.2020.00429.
[13] Wu JH, Xu K, Liu JH, Du LL, Li XS, Su YM, et al. LncRNA MT1JP inhibits the malignant progression of hepatocellular carcinoma through regulating AKT. Eur Rev Med Pharmacol Sci 2020;24:6647–56 doi: 21651 [pii]. https://doi.org/10.26355/eurrev_202006_21651.
[14] Zhu X, Chen F, Shao Y, Xu D, Guo J. Long intergenic non-protein coding RNA 1006 used as a potential novel biomarker of gastric cancer. Cancer Biomark 2017;21:73–80 CBM170273 [pii]. https://doi.org/10.3233/CBM-170273.
[15] Zhang L, Wang Y, You G, Li C, Meng B, Zhou M, et al. LINC01006 promotes cell proliferation and metastasis in pancreatic cancer via miR-2682-5p/HOXB8 axis. Cancer Cell Int 2019;19:320. 1036 [pii]. https://doi.org/10.1186/s12935-019-1036-2.
[16] Guarnieri DJ, DiLeone RJ. MicroRNAs: a new class of gene regulators. Ann Med 2008;40:197–208 788681445 [pii]. https://doi.org/10.1080/07853890701771823.
[17] Wang L, Yao J, Zhang X, Guo B, Le X, Cubberly M, et al. miRNA-302b suppresses human hepatocellular carcinoma by targeting AKT2. Mol Cancer Res 2014;12:190–202 1541-7786.MCR-13-0411 [pii]. https://doi.org/10.1158/1541-7786.MCR-13-0411.
[18] Li F, Wang F, Zhu C, Wei Q, Zhang T, Zhou YL. miR-221 suppression through nanoparticle-based miRNA delivery system for hepatocellular carcinoma therapy and its diagnosis as a potential biomarker. Int J Nanomed 2018;13:2295–307 [pii]. https://doi.org/10.2147/IJN.S157805 ijn-13-2295.
[19] Wang Y, Yang L, Chen T, Liu X, Guo Y, Zhu Q, et al. A novel lncRNA MCM3AP-AS1 promotes the growth of hepatocellular carcinoma by targeting miR-194-5p/FOXA1 axis. Mol Cancer 2019;18:28. 10.1186/s12943-019-0957-7 [pii]. https://doi.org/10.1186/s12943-019-0957-7.
[20] Kong Q, Zhang S, Liang C, Zhang Y, Chen S, Qin J, et al. LncRNA XIST functions as a molecular sponge of miR-194-5p to regulate MAPK1 expression in hepatocellular carcinoma cell. J Cell Biochem 2018;119:4458–68. https://doi.org/10.1002/jcb.26540.
[21] Gao S, Chu Q, Liu X, Zhao X, Qin L, Li G, et al. Long noncoding RNA HEIH promotes proliferation, migration and invasion of retinoblastoma cells through miR-194-5p/WEE1 axis. Onco Targets Ther 2020;13:12033–41 [pii]. https://doi.org/10.2147/OTT.S268942 268942.
[22] Niu X, Nong S, Gong J, Zhang X, Tang H, Zhou T, et al. MiR-194 promotes hepatocellular carcinoma through negative regulation of CADM1. Int J Clin Exp Pathol 2020;13:1518–28.
[23] Gao D, Lv AE, Li HP, Han DH, Zhang YP. LncRNA MALAT-1 elevates HMGB1 to promote autophagy resulting in inhibition of tumor cell apoptosis in multiple myeloma. J Cell Biochem 2017;118:3341–8. https://doi.org/10.1002/jcb.25987.
[24] Bosch FX, Ribes J, Diaz M, Cleries R. Primary liver cancer: worldwide incidence and trends. Gastroenterology 2004;127:S5–S16 S0016508504015902 [pii]. https://doi.org/10.1053/j.gastro.2004.09.011.
[25] El-Serag HB, Rudolph KL. Hepatocellular carcinoma: epidemiology and molecular carcinogenesis. Gastroenterology 2007;132:2557–76 doi: S0016-5085(07)00799-8 [pii]. https://doi.org/10.1053/j.gastro.2007.04.061.
[26] Huang X, Gao Y, Qin J, Lu S. lncRNA MIAT promotes proliferation and invasion of HCC cells via sponging miR-214. Am J Physiol Gastrointest Liver Physiol 2018;314:G559–65 ajpgi.00242.2017 [pii]. https://doi.org/10.1152/ajpgi.00242.2017.
[27] Wang CZ, Yan GX, Dong DS, Xin H, Liu ZY. LncRNA-ATB promotes autophagy by activating Yes-associated protein and inducing autophagy-related protein 5 expression in hepatocellular carcinoma. World J Gastroenterol 2019;25:5310–22. https://doi.org/10.3748/wjg.v25.i35.5310.
[28] D. Cheng, J. Deng, B. Zhang, X. He, Z. Meng, G. Li, et al. LncRNA HOTAIR epigenetically suppresses miR-122 expression in hepatocellular carcinoma via DNA methylation. EBioMedicine 2018:36:159-170. doi: S2352-3964(18)30348-7 [pii] 10.1016/j.ebiom.2018.08.055.
[29] Ma E, Wang Q, Li J, Zhang X, Guo Z, Yang X. LINC01006 facilitates cell proliferation, migration and invasion in prostate cancer through targeting miR-34a-5p to upregulate DAAM1. Cancer Cell Int 2020;20:515. 1577 [pii]. https://doi.org/10.1186/s12935-020-01577-1.
[30] Klingenberg M, Matsuda A, Diederichs S, Patel T. Non-coding RNA in hepatocellular carcinoma: mechanisms, biomarkers and therapeutic targets. J Hepatol 2017;67:603–18 S0168-8278(17)30250-7 [pii]. https://doi.org/10.1016/j.jhep.2017.04.009.
[31] Wang YG, Wang T, Shi M, Zhai B. Long noncoding RNA EPB41L4A-AS2 inhibits hepatocellular carcinoma development by sponging miR-301a-5p and targeting FOXL1. J Exp Clin Cancer Res 2019;38:153. 10.1186/s13046-019-1128-9 [pii]. https://doi.org/10.1186/s13046-019-1128-9.
[32] Ren Y, Shang J, Li J, Liu W, Zhang Z, Yuan J, et al. The long noncoding RNA PCAT-1 links the microRNA miR-215 to oncogene CRKL-mediated signaling in hepatocellular carcinoma. J Biol Chem 2017;292:17939–49 M116.773978 [pii]. https://doi.org/10.1074/jbc.M116.773978.
[33] Zhao ZB, Chen F, Bai XF. Long noncoding RNA MALAT1 regulates hepatocellular carcinoma growth under hypoxia via sponging MicroRNA-200a. Yonsei Med J 2019;60:727–34 60.727 [pii]. https://doi.org/10.3349/ymj.2019.60.8.727.
[34] Faraji F, Pang Y, Walker RC, Nieves Borges R, Yang L, Hunter KW. Cadm1 is a metastasis susceptibility gene that suppresses metastasis by modifying tumor interaction with the cell-mediated immunity. PLoS Genet 2012;8:e1002926 PGENETICS-D-12-01164 [pii]. https://doi.org/10.1371/journal.pgen.1002926.
[35] Mazumder Indra D, Mitra S, Roy A, Mondal RK, Basu PS, Roychoudhury S, et al. Alterations of ATM and CADM1 in chromosomal 11q22.3-23.2 region are associated with the development of invasive cervical carcinoma. Hum Genet 2011;130:735–48. https://doi.org/10.1007/s00439-011-1015-8.
[36] Feng FM, Liu XX, Sun YH, Zhang P, Sun SF, Zhang B, et al. Independent and joint effects of the IL-6 and IL-10 gene polymorphisms in pulmonary tuberculosis among the Chinese Han population. Genet Mol Res 2014;13:7766–72. https://doi.org/10.4238/2014.September.26.14.
[37] Zhang W, Xie HY, Ding SM, Xing CY, Chen A, Lai MC, et al. CADM1 regulates the G1/S transition and represses tumorigenicity through the Rb-E2F pathway in hepatocellular carcinoma. Hepatobiliary Pancreat Dis Int 2016;15:289–96 S1499-3872(16)60099-1 [pii]. https://doi.org/10.1016/s1499-3872(16)60099-1.
[38] Sun Z, Meng C, Wang S, Zhou N, Guan M, Bai C, et al. MicroRNA-1246 enhances migration and invasion through CADM1 in hepatocellular carcinoma. BMC Cancer 2014;14:616. [pii]. https://doi.org/10.1186/1471-2407-14-616 1471-2407-14-616.
[39] Li QJ, Zhou L, Yang F, Wang GX, Zheng H, Wang DS, et al. MicroRNA-10b promotes migration and invasion through CADM1 in human hepatocellular carcinoma cells. Tumour Biol 2012;33:1455–65. https://doi.org/10.1007/s13277-012-0396-1.
[40] Wu DM, Zheng ZH, Zhang YB, Fan SH, Zhang ZF, Wang YJ, et al. Down-regulated lncRNA DLX6-AS1 inhibits tumorigenesis through STAT3 signaling pathway by suppressing CADM1 promoter methylation in liver cancer stem cells. J Exp Clin Cancer Res 2019;38:237. 10.1186/s13046-019-1239-3 [pii]. https://doi.org/10.1186/s13046-019-1239-3.